Aug 20th, 12:00 AM

Impact Loading of Thin-walled Columns

Nishikant R. Vaidya

Charles G. Culver

IMPACT LOADING OF THIN-WALLED COLUMNS

By Nishikant R. Vaidya[1], and Charles G. Culver[2]

INTRODUCTION

Design problems associated with thin-walled members subjected to impact loading arise in connection with transportation related equipment. Several practical examples may be cited; for example, the framework of railway coaches, farm equipment and highway equipment and in some cases even in building construction, especially in small scale structures such as small commercial and manufacturing buildings.

Although the behavior of ordinary hot-rolled shapes subjected to dynamic loading is fairly well understood, these results cannot, however, be extended directly to thin-walled members. The behavior of thin-walled members subjected to impact loading is influenced by local buckling. The effect of the post-buckling strength of the plate elements comprising the cross section is an important design consideration for such members. For computation of the dynamic response therefore, it would be necessary to investigate the interaction between the response of the individual plate elements comprising the cross section and the response of the member as a whole.

A research study on this general problem has been under way since 1967 (1). Details of experimental and analytical studies of structural elements such as thin sheets and thin-walled beams have been reported elsewhere (8,12,13).

The purpose of the present paper is to outline similar work on thin-walled columns. An analytical model is presented for computing the dynamic response of thin-walled columns subjected to axial impact loading. Results obtained from the analysis are compared with experimental values reported by Logue (7). The scope of this paper is limited to short duration impact loading which is defined by prescribing the time variation of the load at the ends of the column.

PROBLEM STATEMENT

Previous investigation of the behavior of columns subjected to dynamic loads dealt primarily with hot rolled shapes or members not subjected to local buckling. Depending on the form of loading, two classes of problems may be distinguished. Problems which deal with periodic loads or loads that are repetitive with time are included in the first class. Important considerations for this class are fatigue failure e.g., bridge structures and the steady state vibration reached after a certain period of time or the loss of stability under periodic loads e.g., structures supporting rotating or reciprocating machinery. The second class of problems includes those that deal with short duration impact loading. Problems associated with this type of loading involve overstressing, large permanent deformations or failure of structural members. The present paper is restricted to the second class of problems. A critical review of both experimental and analytical work pertaining to this class of problems is available elsewhere (7,11).

Although the dynamic response of ordinary columns subjected to impact loading has been investigated both in the elastic and inelastic ranges, no attempt has been made thus far to study the influence of the various parameters on the maximum response. In the present investigation a mathematical model is developed to obtain response spectra or maximum response curves for conditions of impact loading in which the time variation of the load is specified. The response of thin-walled columns in both the elastic and inelastic range is computed.

The definition of the problem in this paper is illustrated in Fig. 1. Fig. 1a shows an initially bent column acted upon by a time varying load. As noted previously, the conditions of impact are defined by prescribing the load at the ends of the column. The particular case considered was that of a triangular load pulse superimposed on an already existing static load. The duration of the load pulses were such that the effect of axial inertia could be neglected and the axial load assumed constant over the whole length of the column. In most structures for which the application of the results of this investigation is contemplated, damping contributes a very small part and hence was not considered in the analysis. Further, shear deformations and rotary inertia have little effect on the overall lateral response of columns of ordinary proportions (3) and therefore were neglected. Small deflection theory was assumed to apply and the curvatures were proportional to the internal moments.

Fig. 1b shows a freebody of a segment of the column at any instant of time. Bearing in mind the assumptions pointed out above, an equilibrium equation can be written in the following form

$$M - P(t) \cdot v - M_e = 0 \qquad (1)$$

In Eq. 1, M = internal resisting moment, P(t) = time varying axial load, v = lateral deflection and M_e = bending moment due to inertia forces. Differentiating Eq. 1 twice with respect to x and recalling that the axial load is a function only of time gives

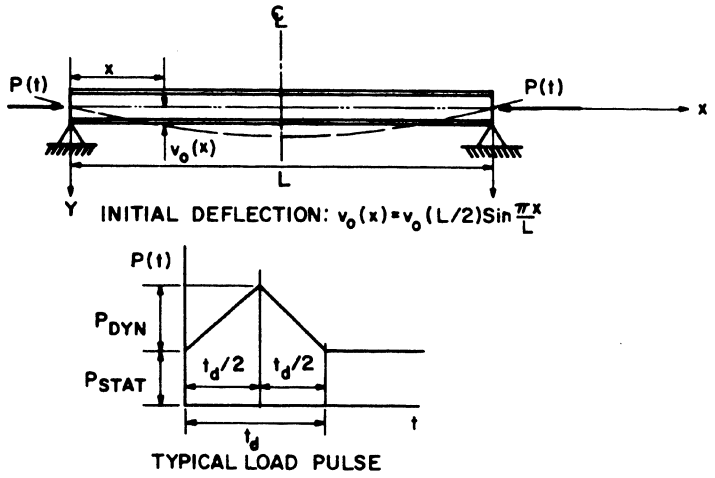

Fig. 1 Problem Statement

[1]Post Doctoral Student, Civil Engineering Department, Carnegie-Mellon University, Pittsburgh, Pennsylvania.

[2]Associate Professor of Civil Engineering, Carnegie-Mellon University, Pittsburgh, Pennsylvania.

[3]Numerals in parentheses refer to corresponding items in Appendix I - References.

$$\frac{\partial^2 M}{\partial x^2} - P(t)\frac{\partial^2 v}{\partial x^2} - \frac{\partial^2 M_e}{\partial x^2} = 0 \qquad (2)$$

In Eq. 2, $\partial^2 M/\partial x^2$ = the lateral resisting force, $\partial^2 v/\partial x^2$ = curvature of the column and $\partial^2 M_e/\partial x^2$ = distributed lateral force due to inertia. Eq. 2 can be put in a more familiar form as follows,

$$\frac{\partial^2 M}{\partial x^2} - P(t)\frac{\partial^2 v}{\partial x^2} - m\frac{\partial^2 v}{\partial t^2} = 0 \qquad (3)$$

where m = mass per unit length and $\partial^2 v/\partial t^2$ = acceleration. Eq. 3 is not readily amenable to a solution as it is. In order to simplify it, the continuous system is idealized by lumped masses and stiffnesses connected by rigid massless bars. Making use of first order central finite difference equations, the following equations result for the i^{th} point,

$$\left.\frac{\partial^2 M}{\partial x^2}\right|_i = \frac{1}{h^2}\left(M_{i-1} - 2M_i + M_{i+1}\right) \qquad (4a)$$

$$\left.\frac{\partial^2 v}{\partial x^2}\right|_i = \frac{1}{h^2}\left(v_{i-1} - 2v_i + v_{i+1}\right) = \phi_i \qquad (4b)$$

where ϕ_i equals the curvature at the point i, and h equals the distance between the mass points, and

$$\left.m\frac{\partial^2 v}{\partial t^2}\right|_i = m\frac{d^2 v_i}{dt^2} \qquad (4c)$$

In order to reduce the number of independent parameters the variables appearing in the equations were nondimensionalized in the following manner,

$$\left.\begin{aligned} \xi_s &= \frac{P_{STAT}}{P_E}, \quad \xi = \frac{P_{DYN}}{P_E}, \quad \beta = \frac{t_d}{t_n} \\ V_i &= \frac{v_i}{v_c}, \quad \tau = \frac{t}{t_d}, \quad \bar{M}_i = \frac{M_i}{M_y} \text{ and } \lambda = \frac{h}{L} \end{aligned}\right\} \qquad (5)$$

where P_E = Euler buckling load = $\pi^2 EI/L^2$, I being the moment of inertia of the original cross section; t_n = period of the fundamental mode of natural vibration of an unloaded column assuming no nonlinear behavior; M_y = moment which causes yielding in the extreme fibers with no axial load and assuming that local buckling does not take place; v_c = centerline deflection corresponding to $M_y = M_y/P_E$; t_d = pulse duration and L = the length of the column.

Using these nondimensional quantities the equation of motion at the i^{th} point is

$$\left(\bar{M}_{i-1} - 2\bar{M}_i + \bar{M}_{i+1}\right) - \left[\xi_s + \xi\,\tau\right]\left(V_{i-1} - 2V_i + V_{i+1}\right) - \frac{m(\lambda L)^2}{P_E t_d^2}\left(\frac{d^2 V_i}{d\tau^2}\right) = 0 \qquad (6)$$

If a similar equation is written for each mass point a system of simultaneous differential equations governing the response results.

If a suitable method of integration and the necessary resistance functions are available Eq. 6 may be readily solved to obtain the dynamic response. Numerical integration techniques are commonly used to solve such equations of motion. These methods essentially consist of reducing the differential equations to a set of algebraic equations by making a suitable assumption for the acceleration over a small time step. The algebraic equations are then solved in each time step and the solution built up by satisfying compatibility of deflection and velocity. Thus this method entails discretizing both the time and space variable.

The method of solution presented herein uses an analog/digital hybrid computer, the integration being performed on the analog and the necessary loading and resistance functions being generated on the digital. The digital computer is used advantageously in high speed computation and generation of arbitrary loading and resistance functions. Performing the integration continuously on the analog overcomes the need for making any kind of approximation for the acceleration thus avoiding truncation errors associated with numerical integration. Since parallel computation is possible on the analog by the use of several components working together, the solution time is at least an order of magnitude smaller than that for an all digital solution. Moreover, insight into the problem is easily gained since there is a direct correspondence between the physical system and its analog. Hence, a more judicious selection of the parameters affecting the solution is possible. Apparently the only major disadvantage offered by the analog computer is its limited equipment capacity. The amount of equipment available permitted a solution of a 5 degree of freedom system. On the basis of the findings of previous investigators (2) this was considered an adequate lumped mass idealization for the continuous system. Further, comparisons with test results and available solutions substantiated this fact.

The task of building an electronic analog for the physical system involves the application of modern analog techniques (4). Interfacing the digital computer with the analog computer is achieved by using such standard equipment as high speed digital to analog and analog to digital converters, operation control lines and sense lines. The analog and logic circuit diagrams are available elsewhere (11).

In order to solve Eq. 6 however, one would require the relation between the internal resisting moments and the curvature which is a function of the deflections at the mass points which are in turn functions of time. In the linear elastic range this relation is proportional to the stiffness, EI, of the column. For the nonlinear range however, this relation is not simple. Nonlinearity may arise either from local buckling which would affect the moment of inertia or from yielding which would change the modulus of elasticity of the yielded portion of the cross section. In both the elastic and inelastic ranges, the relation further depends upon the magnitude of the axial load. In the present analysis the two causes of nonlinearity are considered separately. Thus if local buckling occurs in the elastic range no inelastic behavior is considered and the solution is terminated when the stress at any point in the column reaches the yield stress. This assumption is reasonable since the thin walled members of interest in this study possess very little inelastic postbuckling strength (6). If the plate elements do not locally buckle, the relation between the internal moments and curvatures is extended into the inelastic range.

NUMERICAL RESULTS

For sections in which local buckling does not occur in the elastic range the derivation of the relations between moments and curvatures involves direct application of the principles outlined by Ketter et al., (5). In the present case the cross section is assumed to be free of any residual stress and the yield stress is assumed constant over the whole cross section. Briefly, the methodology used in deriving the moment-curvature relations is to assume an axial load exists on the column then apply a moment and compute the corresponding curvatures assuming that plane sections remain plane. Table 1 shows the dimensions of the cross section which were considered for the development of the M-P-ϕ relations. When the width-to-thickness ratios of the plate elements comprising these cross sections are such that local buckling does not occur, one obtains for the static case a from factor, Q, equal to one (9). The M-P-ϕ relation for sections with Q = 1, for bending about the strong axis match those derived for a hot-rolled shape without residual stress (5). For bending about the weak axis however, they differ somewhat. This is due to the fact

TABLE 1

DIMENSIONS OF SECTIONS CONSIDERED FOR DEVELOPING THE M-P-ϕ RELATIONS

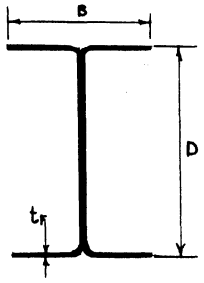

SECTION	B (IN)	D (IN)	t_F (IN)	(w/t) FLANGE	(w/t) WEB	Q
1	1.50	1.50	0.068	8.7	17.3	1.0
2	2.75	3.00	0.015	10.3	23.0	1.0
3	3.00	5.00	0.135	8.7	32.3	1.0
4	3.00	4.00	0.068	19.6	54.0	0.790
5	5.00	5.00	0.060	39.1	78.2	0.391
6	6.00	8.00	0.075	37.8	102.3	0.405

that for the section considered here the web contributes appreciably to the internal moment. Its effect was considered in developing the moment-curvature relations herein whereas Ketter, et al. neglected the web.

Sections in which local buckling takes place in the elastic range are characterized by a form factor Q < 1 (9). Table 1 shows the dimensions of such sections considered for developing the M-P-ϕ relations. For these sections two distinct stress conditions can exist; one where the total stress on the elements is less than their buckling stress and the other where the stress is above that which causes these elements to buckle. In the former condition, the moments and curvatures are linearly related by the stiffness, EI, of the column. For the latter condition, the concept of effective width is used where a stress above the local buckling stress is allowed to exist and effective widths computed on the basis of the width-to-thickness ratios of the elements (9,10). The flanges are assumed to have one edge simply supported and the other edges free, whereas the webs are assumed to be simply supported on both longitudinal edges. The computation of the section properties such as area and moment of inertia involve an iterative procedure since the stress condition must reflect the reduced sectional area and moment of inertia. Fig. 2a shows the stress condition under an axial load which produces local buckling in both the web and the flanges. An iterative procedure is used to obtain the true magnitude of the uniform stress under this axial load alone. After this is done the stress on the compression flange is incremented by a certain amount, f_{INCR}. Correspondingly, a new effective width of the compression flange results. Keeping the total stress on the compression flange constant, the effective widths of the web and bottom flange are adjusted by an iterative procedure. After the correct effective widths are obtained, the moments and curvatures are computed by satisfying the following relations

$$P = \int_{A_{eff}} \sigma dA \quad ; \quad M = \int_{A_{eff}} \sigma y dA$$

A more detailed description of the development of the moment-axial load-curvature relations is given elsewhere (11). Fig. 3 shows the M-P-ϕ curves derived in the manner explained above for a 5" x 5" x 16 ga. sec-

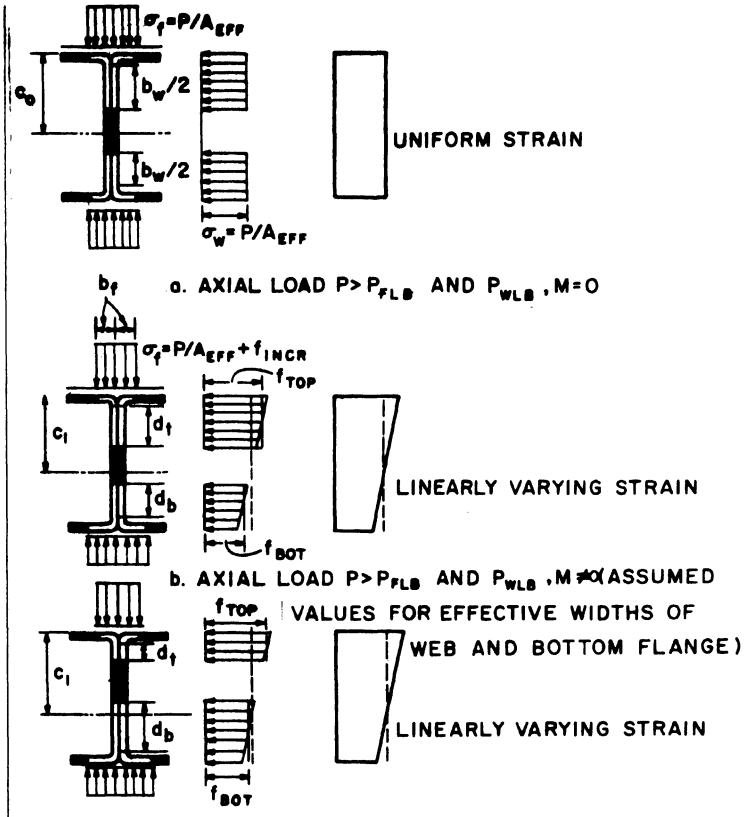

Fig. 2 Stress and Strain Distribution Over Cross Section
P > Local Buckling Load

tion, for bending about the strong axis. The flanges have a width-to-thickness ratio of 39.1 and the webs, 78.2. This section is characterized by a form factor, Q = 0.391. For low values of axial load the M-ϕ curves start off linear with a slope equal to the original stiffness, EI, of the column. This trend continues until the stress on the compression flange equals the buckling stress for that element. Beyond this value of stress the section properties such as area and moment of inertia are reduced. This is reflected in a change in the slope of the M-ϕ curve. Any additional increment in stress on the compression flange entails computation of a new value of the effective area, the moment of inertia and the position of zero bending strain. Consequently the relation between the moments and curvatures is no longer linear. For values of $\bar{P}$ = P/P_y greater than 0.3 the M-ϕ curves are nonlinear from the beginning of loading and the initial slope is different from the original stiffness of the column. This is due to the fact that the column locally buckles under the axial load alone. As may be expected the extent of deviation from linearity is influenced by the width-to-thickness ratios of the plate elements i.e., the flanges and web.

The M-P-ϕ relations for sections with Q < 1 not only depend upon the value of the form factor but also the width-to-thickness ratios of the plate elements. This fact was borne out by comparison of the M-ϕ relations for two sections which have approximately the same value of form factor, Q, computed by the method outlined in the AISI Specification (9). An M-ϕ relation was developed for each section for a value of $\bar{P}$ equal to 0.6. As shown in Fig. 4, the M-ϕ relations for the two sections differ substantially. Hence no conclusion can be drawn as to the general applicability of the M-P-ϕ relations for cross sections with Q < 1, even

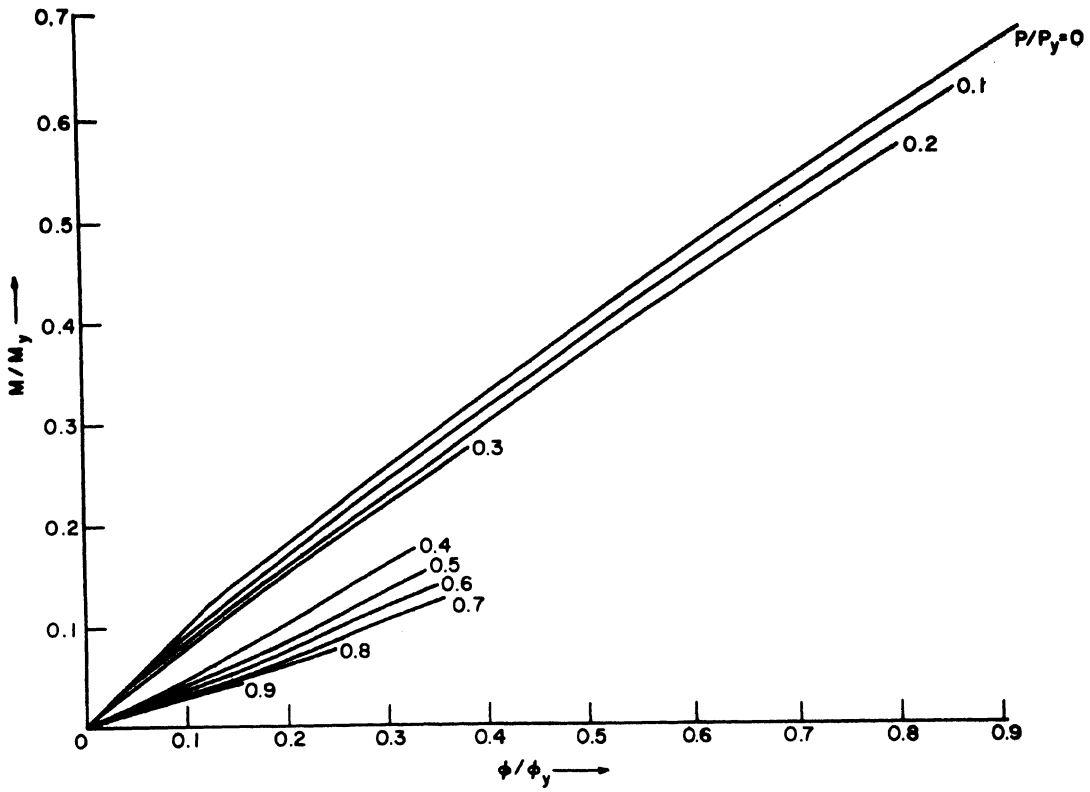

Fig. 3 Moment-Axial Load-Curvature Relations for 5" x 5" x 16 ga. Section (Strong Axis Bending)

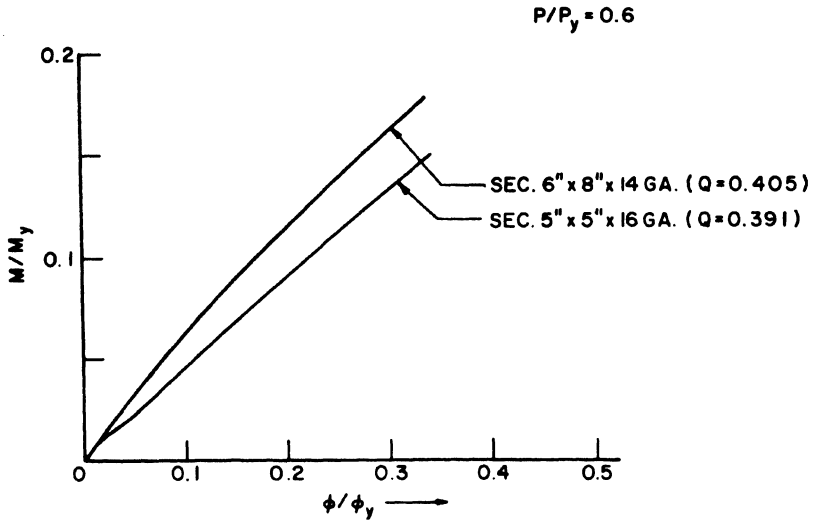

Fig. 4 Comparison of Moment-Curvature Relations, Q = 0.4 (Strong Axis Bending)

when the value of the form factor is the same.

The M-P-ϕ relations thus derived are stored in the digital computer and used in the solution of Eq. 6 to obtain the internal moments from known curvatures. As pointed out above these relations depend upon the magnitude of the axial load on the column. Thus at any instant of time the internal moment is a function of two variables, one the curvature and the other the axial load. Since the axial load on the column varies in a continuous fashion the moment-curvature relations used to compute the internal moments would have to vary continuously to include the whole spectrum of values of axial loads encountered. However, it is difficult if not impossible to express the moment-axial load-curvature relations in a continuous fashion. Since these were computed only for discrete values of the axial load, an interpolation scheme was necessary to compute the moment-curvature relations for intermediate values of axial load. This procedure entailed discretizing the loading function. To facilitate the computation of moment-curvature relations for intermediate values of axial loads, the triangular load pulse is approximated by a series of step pulses. In each step the magnitude of the applied axial load being constant, the corresponding relation between moment and curvature is defined. Eq. 6 can therefore be readily solved. This is done for each step separately using as the initial conditions the deflections and velocities at the end of the preceding step. Convergence of the solution thus obtained was insured by comparing it with a solution for a true triangular pulse.

To check the validity of the model developed herein, the solutions obtained from it were checked with some existing solutions. For the

elastic case, the solution for a constant magnitude force pulse obtained from the hybrid model was compared with a normal mode superposition solution. Also the inelastic response of a particular column investigated by Hartz and Clough (2) was compared with their test results. Very good correlation was obtained for both these cases (11).

The validity of the model developed herein was further checked by comparing the analytical results with experimental values obtained during a series of dynamic tests performed by Logue (7). Table 2 shows this comparison. Note that the dynamic deflections measured during the tests were fairly small. This was attributed to the small initial imperfections existing in the test specimens. This fact, i.e. the small dynamic deflections, substantiated the analytical results since the computed values of dynamic deflections, δ_{DYN} were also small. Fairly good correlation was obtained between analytical and experimental results. The analytical

TABLE 2

COMPARISON WITH TEST RESULTS

$1\frac{1}{2}$" x $1\frac{1}{2}$" SECTION

SPECIMEN	SLENDERNESS RATIO	TEST NO.	TEST RESULTS		ANAL. RESULTS		% GREATER THAN TEST	
			δ_{DYN} (IN)	λ_{DEF}	δ_{DYN} (IN)	λ_{DEF}	δ_{DYN}	λ_{DEF}
B-40-D	48.56	1	0.0010	1.12	0.0 12	1.3119	+20.0	+17.10
		2	0.0007	1.26	0.0007	1.2447	0.0	- 1.22
		3	0.0020	1.04	0.0023	1.1914	+15.0	+14.57
B-60-D	58.93	1	0.0006	1.49	0.0007	1.6414	+16.67	+10.16
		2	0.0009	1.32	0.0008	1.2969	-11.11	- 1.75
		3	0.0004	1.02	0.0004	1.0142	0.0	- 0.57
B-80-D	86.18	1	0.0007	1.80	0.0008	1.9739	+14.30	+ 9.65
		2	0.0014	1.75	0.0014	1.6974	0.0	- 3.02
		3	0.0028	1.53	0.0030	1.6064	+ 7.15	+ 5.00
		4	0.0033	1.23	0.0036	1.3390	+ 9.10	+ 8.78
		5	0.0048	1.07	0.0052	1.1586	+ 8.34	+ 8.23
B-120-D	125.58	1	0.0059	1.64	0.0067	1.8625	+13.58	+13.58
		2	0.0055	1.96	0.0062	2.2306	+12.71	+13.80
		3	0.0080	1.54	0.0083	1.5907	+ 3.75	+ 3.30
		4	0.0125	1.49	0.0129	1.5350	+ 3.20	+ 3.02
		5	0.0163	1.46	0.0158	1.4176	- 3.07	- 2.90
		6	0.0175	1.28	0.0195	1.4223	+11.41	+11.12

results were, in most cases, greater than those obtained experimentally. Similar comparisons with test results for columns with $Q < 1$ are presented elsewhere (11).

The model developed herein was used to obtain the dynamic response, i.e. the centerline deflection of a column. Previous studies indicated that the following parameters affect the dynamic response of simple structures subjected to impact loading: shape of loading pulse, load magnitude and load duration. In view of the scope of the present study it was deemed necessary to include the following additional parameters: static preload, initial imperfection, and dimensions of the cross section. As pointed out earlier the only form of impact considered was that of a triangular load pulse. No attempt was made to investigate the effect of the shape of the loading pulse.

The deflection response of a pinned-end column subjected to impact loading is shown in Figs. 5 through 8. The deflection at the midpoint of the column is plotted as a function of the nondimensional time. These plots were recorded directly from the analog computer.

Results from the dynamic response calculations indicated that the deflection lags the applied dynamic load, i.e. the maximum deflection occurs after the load has reached its maximum and is decreasing. This is due to the fact that in the initial stages of loading the lateral inertia forces tend to make the column "stiffer" thereby resisting its outward movement. The time lag between the maximum applied load and the maximum response depends upon the rate of application of the load. As the rate increases this time lag becomes larger. In the extreme case of static loading which can be simulated by a very low rate of loading, the deflections keep up with the load and consequently the time lag between the maximum load and miximum deflection reduces to zero. In the present investigation the rate of loading is represented by the nondimensional pulse duration β.

Fig. 5 shows the effect of the pulse duration on the dynamic response of an initially bent column. The particular case considered is a column with a slenderness ratio of 120.0 carrying a static preload equal to 51% of the Euler buckling load, $\xi_s = 0.51$. The impact load is in the form of a triangular load pulse with the maximum dynamic load being equal to 30% of the Euler load, $\xi = 0.30$. The peak dynamic load occurs at $t/t_d = 0.5$. As seen from Fig. 5 the time lag between the maximum deflection and the maximum load decreases as the magnitude of the pulse duration increases. Also the maximum dynamic deflection reached by the column is a function of the load duration. For short durations of the loading pulse ($\beta < 1.0$) the maximum amplitude of the lateral vibrations on the second and third cycles is approximately equal to the maximum deflection recorded during the first cycle during load application. The column eventually vibrates about its equilibrium position under the axial load with a frequency equal to the natural frequency of the column carrying a static load. For larger values of β, however, the maximum amplitudes on the second and third cycle fall below the maximum deflection recorded during the first cycle.

Fig. 6 shows the effect of the magnitude of the maximum dynamic load on the lateral response of the column. Note that the time at which the maximum deflections occur are not identical for the three values of ξ considered. As the magnitude of ξ increases the peak deflection occurs later in time. Although the difference is very small, this fact gives an indication of the nonlinearity introduced due to the applied load. As in the above case, after the dynamic load is off the column it eventually vibrates about its equilibrium position under the static load.

The influence of the magnitude of the static preload is shown in Fig. 7. The response for a particular column subjected to a maximum dynamic load equal to 30% of the Euler buckling load and a ratio of load pulse duration to the natural period of the unloaded column equal to 4.0 is shown. Three different values of static loads are considered. The initial deflections for the three loads were the same and are those present under the static load alone. The ensuing free vibrations after the dynamic load equals zero differ in both their amplitude and frequency. The response curves in this time range reflect the amount of static load present on the column. As the magnitude of the static preload increases the nonlinearity introduced by it increases. This is due to the fact that the static load deflection curve of a column is more nonlinear for higher loads. As the nonlinearity becomes greater the time lag for deflections increases and the lateral response for columns supporting larger static loads tends to peak at a later time.

It is interesting to note that for small initial deflections the time lag between the peak response and the maximum dynamic load is greater than for larger values of initial deflections. This fact can be observed

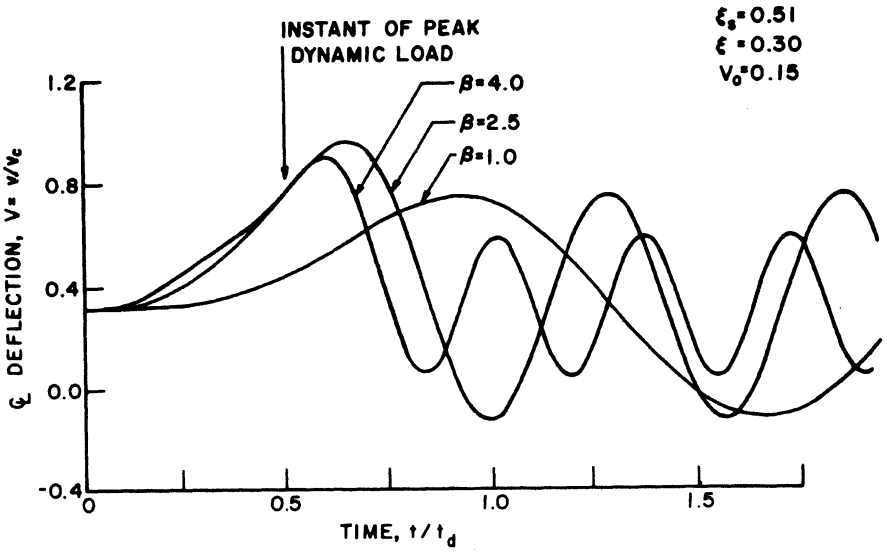

Fig. 5 Effect of Pulse Duration on the Dynamic Response

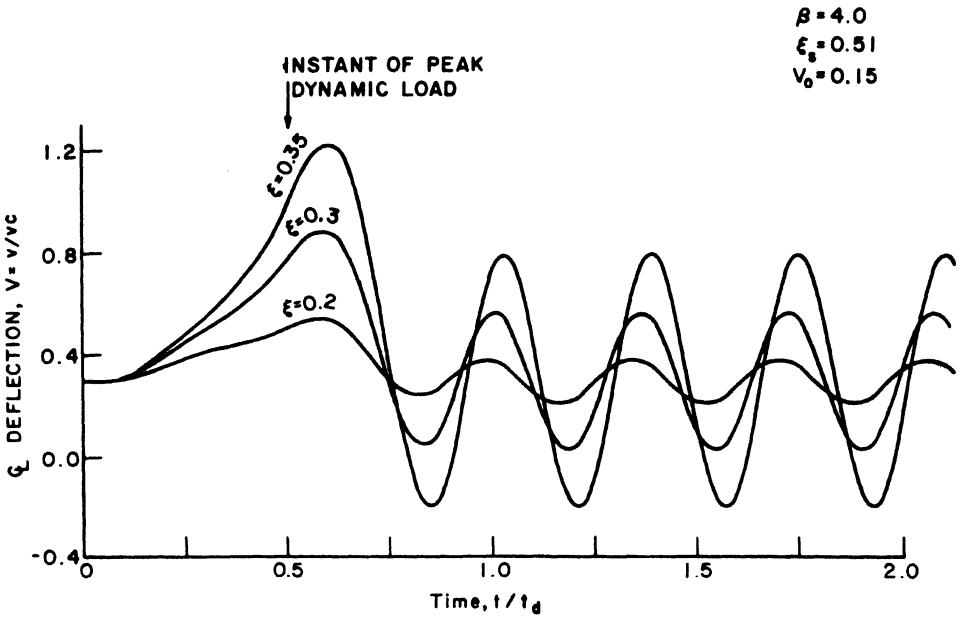

Fig. 6 Effect of the Maximum Dynamic Load on the Dynamic Response

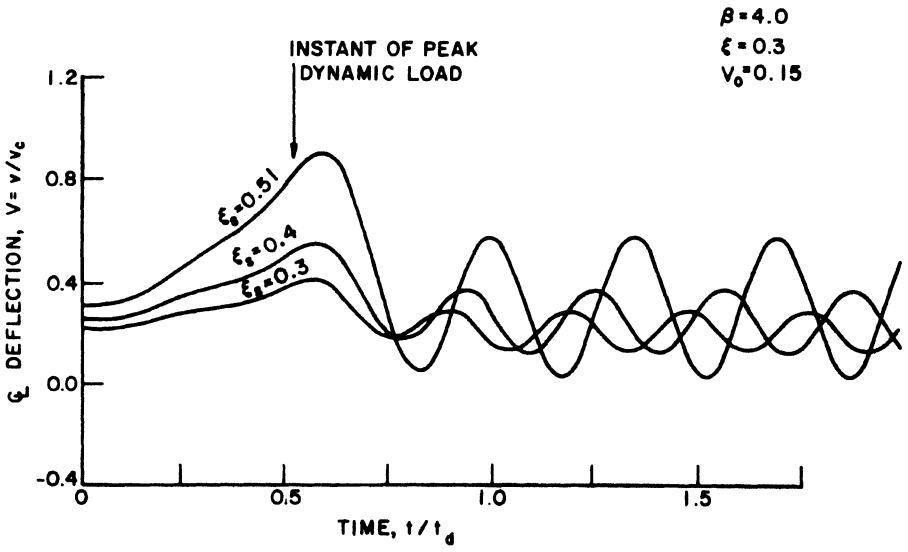

Fig. 7 Effect of Static Preload on the Dynamic Response

in Fig. 8 which shows the effect of the initial imperfections on the lateral response of a column. Three values of initial imperfections are considered, the shape of this initial deflection being the same for all three cases, viz., a sine curve. The peak response is greatest for the largest value of the initial imperfection. The frequency of the ensuing free vibrations, however, is identical for all the three cases since this depends only on the magnitude of the static load present.

The maximum response reached during the lateral motion of the column is of primary interest to the designer. Response spectra were therefore plotted by recording the maximum deflections obtained for several loading cases. The influence of the various parameters such as the static load, the dynamic load, pulse duration and the initial imperfection on the response spectra was investigated.

Fig. 9 shows the elastic response spectra for a column with cross sectional dimensions of $1\frac{1}{2}$" x $1\frac{1}{2}$" x 16 ga. The static preload in this case equals the design load for the column with a slenderness ratio of 120 (9). Note that since the loading parameters are nondimensionalized with respect to the Euler buckling load the slenderness ratio does not enter directly as a parameter affecting the solution. In other words, for any other length of the column, the response spectra with a static preload of 51% of the Euler buckling load would be identical provided the column remained elastic. As seen from Fig. 9 for larger magnitudes of peak dynamic load the maximum response is obtained for greater values of the nondimensional pulse duration β. This reflects the nonlinearity introduced due to the nonlinear load-deflection relation. Note that as the magnitudes of the peak dynamic load increase, the value of the nondimensional maximum dynamic deflection decreases. The incremental dynamic deflection, δ_{DYN}, is nondimensionalized with respect to δ_{STAT} which is the incremental static deflection produced if the peak dynamic load is applied statically. Similar response spectra were obtained for several other loading cases (11).

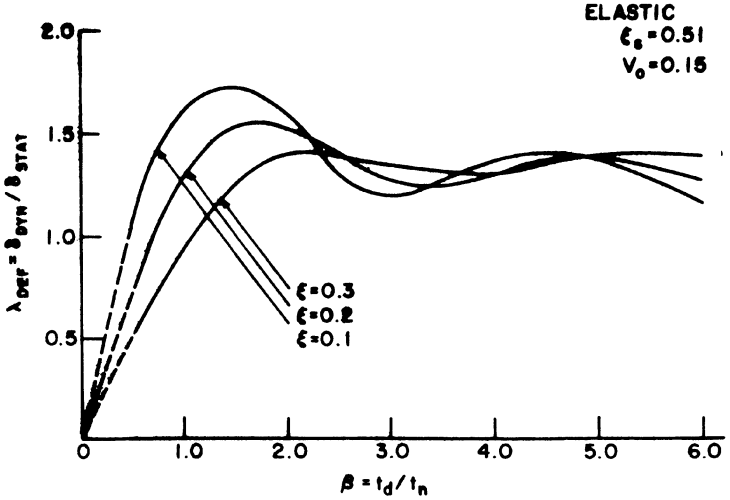

Fig. 9 Response Spectra for Deflection

SUMMARY AND CONCLUSIONS

A mathematical model was presented for the solution of the dynamic response of thin-walled columns subjected to impact loading defined by prescribing the load at the ends of the column. The particular form of impact loading considered was that of a triangular load pulse superimposed on an already existing static load. Nonlinearity due to local buckling was accounted for by using nonlinear moment-axial load-curvature relations derived with the aid of the effective width concept. The equations of motion were solved using an analog/digital hybrid computer.

The effect of various parameters such as the peak dynamic load, pulse duration, static preload and initial imperfection on the dynamic response was investigated. For design purposes the maximum response reached during the lateral motion of the column or failure of the column are important considerations. Response spectra or maximum response curves and failure envelopes were also obtained (11). These will be discussed in subsequent publications.

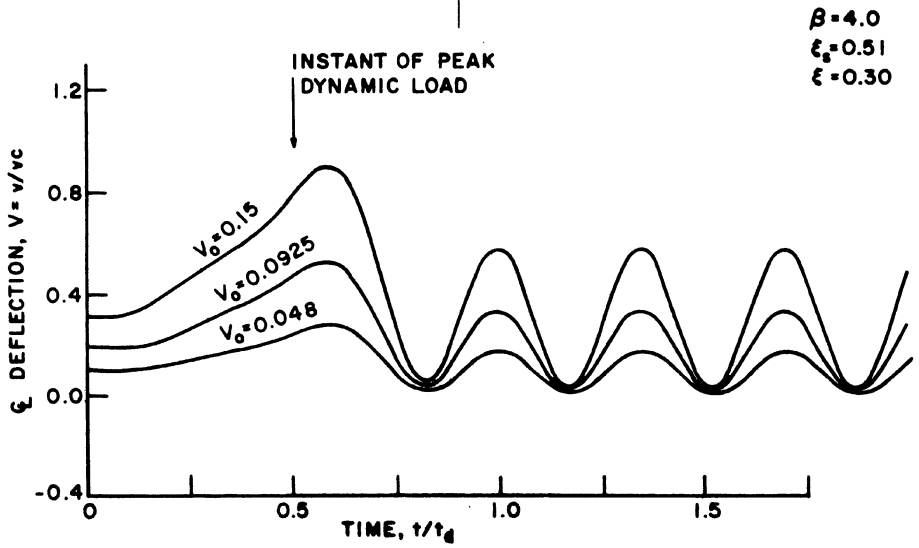

Fig. 8 Effect of Initial Deflection on the Dynamic Response

ACKNOWLEDGMENTS

The results presented herein were taken from a doctoral thesis submitted by Nishikant R. Vaidya to the Department of Civil Engineering, Carnegie-Mellon University. This research was undertaken under the guidance of Charles G. Culver. This work represents the third and the last phase of a research program on "Light Gage Cold-Formed Structural Elements Subjected to Time-Dependent Loading" sponsored by the American Iron and Steel Institute at Carnegie-Mellon University. The cooperation of W. G. Kirkland, Vice President, AISI, and the members of the AISI task group on the Influence of Dynamic Loading on Structural Behavior of Light Gage Steel, R. B. Matlock, Chairman, J. B. Scalzi and C. R. Clauer is gratefully acknowledged. Comments provided by A. L. Johnson and J. J. Healey of AISI in reviewing the technical reports on this project are also acknowledged.

APPENDIX I - REFERENCES

1. Culver C., "Impact Loading of Cold-Formed Steel Members," Preprint 1232, presented at the ASCE National Meeting on Transportation Engineering, Boston, Massachusetts, July 13-17, 1970.

2. Hartz, B. J., and Clough, R. W., "Inelastic Response of Columns to Dynamic Loading," Journ. of the Engineering Mechanics Div., ASCE, April 1957, pp. 1-14.

3. Housner G. W., and Tso, W. K., "Dynamic Behavior of Supercritically Loaded Struts," Journ. of the Engineering Mechanics Div., ASCE, EMS, Vol. 88, October 1962, p. 41.

4. Johnson, C. L., "Analog Computer Techniques," McGraw-Hill Book Co., New York, N. Y., 1956.

5. Ketter, R. L., Kaminsky, E. L., and Beedle, L. S., "Plastic Deformation of Wide Flange Beam-Columns," Transactions, ASCE, Vol. 120, 1955, p. 1028.

6. Light Gage Cold-Formed Steel Design Manual, American Iron and Steel Institute, New York, 1962.

7. Logue, J. M., "Experimental Study of Thin-Walled Columns Subjected to Impact Loading," thesis submitted to Carnegie-Mellon University, Pittsburgh, Pennsylvania, 1971, in partial fulfillment of the requirements for the degree of Master of Science.

8. Osgood, A., "Response Spectra for Light Gage Cold-Formed Beams," thesis submitted to Carnegie-Mellon University, Pittsburgh, Pennsylvania, 1969, in partial fulfillment of the requirements for the degree of Master of Science.

9. Specification for the Design of Cold-Formed Steel Structural Members, American Iron and Steel Institute, New York, 1968.

10. Uribe, J., and Winter, G., "Aspects of the Effects of Cold-Forming on the Properties and Performance of Light-Gage Structural Members," Cornell Univ. Report submitted to the American Iron and Steel Institute, Report no. 333, Ithaca, N. Y., May 1969.

11. Vaidya, N. R., "Response of Thin-Walled Columns Subjected to Impact Loading," thesis presented to Carnegie-Mellon University, Pittsburgh, Pennsylvania, 1971, in partial fulfillment of the requirements for the degree of Doctor of Philosophy.

12. Van Tassel, R., "Large Deflection Theory for Plates Subjected to Dynamic Edge Loading," thesis presented to Carnegie-Mellon University, Pittsburgh, Pennsylvania, 1968, in partial fulfillment of the requirements for the degree of Doctor of Philosophy.

13. Zanoni, E. A., "Nonlinear Analysis of Light-Gage Cold-Formed Beams Subjected to Shock Loading," thesis presented to Carnegie-Mellon University, Pittsburgh, Pennsylvania, 1969, in partial fulfillment of the requirements for the degree of Doctor of Philosophy.

APPENDIX II - NOTATION

A_{eff} = Effective area of cross section, $in.^2$;

B = Overall width of cross section, in.;

b_f = Effective width of flanges, in.;

b_w = Effective width of web, in.;

c_o = Distance of centroid from top of cross section, in.;

c_1 = Distance of the point of zero bending strain from top of cross section, in.;

D = Overall depth of cross section, in.;

d_b = Effective width at bottom of web, in.;

d_t = Effective width at top of web, in.;

E = Elastic modulus, $K/in.^2$;

f_{BOT} = Average stress on bottom portion of web, Ksi;

f_{INCR} = Stress increment at extreme fiber, Ksi;

f_{TOP} = Average stress on top portion of web, Ksi;

h = Distance between mass points, in.;

I = Moment of inertia of original section;

i = Mass point designation;

L = Column length, in.;

M = Internal moment K-in.;

M_e = Moment due to inertia forces, K-in.;

M_i = Internal moment at the i^{th} point, K-in.;

M_y = Yield moment with zero axial load on column, K-in.;

$\bar{M}$ = Ratio of internal moment to yield moment, M/M_y;

m = Mass of column per unit length, $lbs.-sec.^2/in./in.$;

P_{DYN} = Maximum dynamically applied load, Kips;

P_E = Euler buckling load = $\pi^2 EI/L^2$, Kips;

P_{FLB} = Axial load which initiates local buckling in flanges = $\sigma_{FLB} A$, Kips;

P_{STAT} = Static preload, Kips;

P_{WLB} = Axial load which initiates local buckling in web = $\sigma_{WLB} A$, Kips;

P_y = Yield load = $\sigma_y \cdot A_{EFF}$, Kips;

$\bar{P}$ = Ratio of total axial load to yield load = P/P_y;

Q = Stress and/or area factor to modify allowable axial stress;

t = Time in sec.;

t_d = Pulse duration in secs.;

t_F = Thickness of plate elements, in.;

t_n = Natural period of vibration of an unloaded column, sec./cy.;

V = Ratio of the total lateral deflection to v ;

$V_o(x)$ = Ratio of initial deflection to v_c;

v_c = Nondimensionalizing parameter for lateral deflection, = M_y/P_E, in.;

v_i = Lateral deflection at the i^{th} point, in.;

$v_o(x)$ = Initial deflection of the column, in.;

w = Flat width of plate element, in.;

x = Distance along the length of the column, in.;

β = Ratio of pulse duration to the natural period of unloaded column;

δ_{DYN} = Maximum deflection under P_{DYN} applied dynamically and P_{STAT} applied statically, K-in.;

δ_{STAT} = Deflection due to P_{DYN} and P_{STAT} applied statically, in.;

σ_y = Yield stress, Ksi;

ϕ = Curvature, in./in.;

ϕ_i = Curvature at the i^{th} point, in./in.;

ϕ_y = Curvature corresponding to M_y, in./in.;

$\bar{\phi}$ = Ratio of curvature to yield curvature, ϕ/ϕ_y;

λ = Ratio of the distance between mass points to the total length of column;

λ_{def} = $\delta_{DYN}/\delta_{STAT}$;

ξ = Ratio of maximum dynamic load to Euler load;

ξ_s = Ratio of static preload to Euler load;

τ = Ratio of time to the pulse duration;